Int. J. Electrochem. Sci., 17 **(2022)** Article Number: 220115, doi: 10.20964/2022.01.03

International Journal of
ELECTROCHEMICAL
SCIENCE
www.electrochemsci.org

Short Communication

First Principles Investigation of NASICON-Structured $LiTi_2(PO_4)_3$ and $Mg_{0.5}Ti_2(PO_4)_3$ Solid Electrolytes

A.M.A Fami[1], N.A Wahab[1], M.S.A. Rani[2], M.K Yaakob[1,3], N.A Mustaffa[1,]*

[1] Faculty of Applied Sciences, Universiti Teknologi MARA, 40450 Shah Alam, Selangor, Malaysia
[2] School of Materials and Mineral Resources Engineering, Universiti Sains Malaysia, 14300 Nibong Tebal, Pulau Pinang, Malaysia
[3] Ionics Materials & Devices (iMADE) Research Laboratory, Institute of Science, Universiti Teknologi MARA (UiTM), 40450, Shah Alam, Selangor, Malaysia
[*]E-mail: nuramalina@uitm.edu.my

Received: 9 September 2021 / *Accepted:* 20 October 2021 / *Published:* 6 December 2021

The structural and electronic properties of NASICON-Structured $LiTi_2(PO_4)_3$ and $Mg_{0.5}Ti_2(PO_4)_3$ were studied by performing first-principles Density Functional Theory (DFT) calculations. Geometrical optimization was conducted before the primitive cell of these structures by using different exchange-correlation energy functional. The Local Density Approximation (LDA) and Generalized-Gradient Approximation functional with Perdew-Burke-Ernzerhof (GGA-PBE) were used to execute structural and electronic properties for both materials. Calculated structural parameters and electronic properties such as band gap, the electronic density of states, and the partial density of states were presented.

Keywords: first-principles investigation, density functional theory, NASICON-structured, structural properties, electronic properties

1. INTRODUCTION

The battery is a storage device for electrochemical energy that consists of converting chemical energy to electrical energy and is known as a small reactor leading to the production of energetic electrons flow through external devices. Its basic construction consists of a porous insulator that distinguishes two metals or compounds with different chemical potentials. These two metals are the anode, which loses electrons while discharging, and cathodes, which accept electrons. The battery can be divided into two types which are non-rechargeable batteries (primary) and rechargeable batteries (secondary). Primary batteries are designed to be used once and should be discarded after being used. The electrochemical reaction in this cell is irreversible. Unlike primary batteries, secondary batteries

can be used more than once as it is being recharged. They can be recharged by having a passing current in the opposite direction of the discharge cycle [1]. Examples of primary batteries are lithium, zinc, and mercury, while secondary batteries are lead-acid, lithium-ion, and lithium metal is not only being used as power sources for electronic gadgets, but it also plays a vital role as high-energy capacity components for electric vehicles and electrical storage systems [2]. Availability of suitable technology for batteries as energy storage is required for electricity production since the sources of sustainable energy vary as time goes by. Therefore, there has been impressive progress in innovative batteries recently as the industry is working towards sustainable development, which means the involvement of energy sources in producing electricity is safe and causing less pollution.

Lithium-ion battery receives tremendous attention from scientific researchers. This may be ascribed to its apparent advantages and promising properties such as high output voltage in the average of 3.2 V to 3.3 V and high energy density, greater than 180 Wh kg^{-1} [3]. In addition, it is better than other chemistries due to its smallest ionic radii, which allows Li-Based batteries to have high gravimetric and volumetric capacity at 3861 $mAhg^{-1}$ and 2062 $mAhcm^{-3,}$ respectively [4]. Lithium (Li) metal as anode leads lithium-ion batteries to reveal their lowest electrochemical potential and highest specific capacity [5]. Li-ion battery technology significantly influences the electrification of mobility and renewable energy sectors, which currently rely on resources that are either unequally distributed in geography or limited in the amount [6]. It is prominent in portable communication equipment and electric vehicles due to its excellent cycling stability and better rate capability [7]. In addition, it provides the facility of minimizing the weight and size of applications, including offers the designers new prospects due to its excellent shelf life [8]. The lithium-ion battery is a better option than the traditional lithium battery. It has been used in many products recently, such as consumer electronics and stationary energy systems. It has become the primary power source due to its outstanding features and is required to maintain its performance and affordable to compete in the market [3]. Due to the qualities that existed in the lithium-ion battery, it has been tested widely [9]. Despite being the manufacturers' first choice, the lithium-ion battery still has drawbacks that stimulate the researchers to study other ionic materials as its replacement. Inadequate amount of lithium available as raw materials leads to failure of sustaining its energy and power to fulfill technology's needs as they are demanded by their applications [10, 11]. The lithium-ion battery is not capable of meeting the industries' requirements even though immense progress has been made yet limited success achieved.

A potential competitor and superior replacement for lithium-ion is magnesium. It can be attributed to its prominent characteristics, such as high energy density, low costs, and less dangerous material [12]. Magnesium is better than lithium because it has higher volumetric gravity and a smaller atomic radius [13]. It has a gravimetric and volumetric capacity of 3833 $mAhg^{-1,}$ and 2062 $mAhcm^{-3,}$ respectively which are higher in value than lithium [6]. With an appropriate design of the electrolyte-cathode system, one can have magnesium batteries with an energy density of 320 Wh kg^{-1} due to divalent properties in Mg^{2+} in oxidation that provides two-electron per metal, unlike one electron in the case of Li. According to a study done in 2012, high ion charge carrier concentration is one of the critical elements that causes high ionic conductivity in materials [14]. Theoretically, Mg^{2+} has a higher ion charge carrier concentration as it is a divalent ion, and it may have better ionic conductivity than monovalent ion like Li^{+}. Magnesium is remarkable for being less reactive, which alleviates restrictions,

especially on manufacturing and safety. Magnesium earned popularity and is an alternative system that propounds excellent economical solutions for electrical storage and suits many potential applications [15].

NASICON stands for Sodium Super Ionic Conductor, categorized under solid oxide electrolytes recognized as promising candidates as solid electrolytes of all-solid-state rechargeable batteries due to high ionic conducting and insulation properties [16]. It has a polyanionic framework focused on by researchers due to its stable 3D crystal structure and other operating capabilities [17]. $A_xM_2(XO_4)_3$ is the general stoichiometry of NASICON where A is alkaline and alkaline-metal, M is metal like Ti, and X is metalloid such as phosphorus, P. Jian et al. stated that various structures could be formed from the exact composition of NASICON compound which enables them to have different chemical properties [18]. The 3D frame comprises A- ions, two MO_6 octahedral, and three PO_4 tetrahedral linked by corner-sharing oxygen to form a network structure named $R\bar{3}C$ [19, 20]. The path along sites A1-A2-A1 are called bottlenecks, but it was unambiguously extracted as the most favorite pathway for the diffusion of Na^+ while TiO_6 octahedral and PO_4 tetrahedral control the effective width of bottlenecks, which affect the hopping rate of A-ions [21]. This compound face difficulties in increasing its ionic conductivity, which reported by previous researchers that the ionic conductivity is between ~ 10^{-7} S cm^{-1} and ~ 10^{-10} S cm^{-1} [22]. $LiTi_2(PO_4)_3$ or Lithium titanium phosphate (LTP) is an example of NASICON-type promising conductive solid electrolyte studied in solid-state lithium batteries due to its advantages. However, its ionic conductivity decreased because the skeleton of NASICON is too large for the migration of Li^+. Choosing a smaller size ion such as Mg^{2+} is a better choice as the atomic radii difference is small, and it has higher ionic conductivity. $Mg_{0.5}Ti_2(PO_4)_3$ (MTP) is a new member of NASICON with low thermal expansion that was prepared by the sol-gel method and investigated as a magnesium host [12]. According to Anuar et al., NASICON is a promising host for the transportation of Mg^{2+} ions. It has excellent structural stability due to its large interstitial void that can uptake guest species. Furthermore, they can transport a charge carrier in the compound, which is an important requirement for electrolytes in battery systems [23].

To the best of our knowledge, no investigation has been reported regarding the first-principle study of $Mg_{0.5}Ti_2(PO_4)_3$. Structural and electronic properties of $LiTi_2(PO_4)_3$ and $Mg_{0.5}Ti_2(PO_4)_3$ can be predicted using a first-principle calculation based on density functional theory (DFT). Crystallographic data obtained from Rietveld refinement analysis of previous studies were used to construct relevant structures of these materials. Geometrical optimization on primitive unit cell is conducted by implementing different correlation energy functions such as local density approximation (LDA), generalized-gradient approximation functional with Perdew-Burke-Ernzerhof (GGA-PBE), and GGA-PBE function for solid (GGA-PBEsol) to choose the best functional approximation to examine the electronic properties of $LiTi_2(PO_4)_3$ and $Mg_{0.5}Ti_2(PO_4)_3$.

2. EXPERIMENTAL

2.1. Computational Method

First-principles calculations of density functional theory on structural and electronic properties of NASICON-structured materials, $LiTi_2(PO_4)_3$ and $Mg_{0.5}Ti_2(PO_4)_3$ was performed using a

computational material science software (Material Studio). This software consists of an MS visualizer for structure modelling and an MS Cambridge Serial Total Energy Package (CASTEP) computer code for geometrical optimization calculation, structural and electronic properties. Crystallographic data from previous studies were used as a reference for modelling of $LiTi_2(PO_4)_3$ (LTP) and $Mg_{0.5}Ti_2(PO_4)_3$ (MTP) [20]. Local Density Approximation (LDA) and Generalized Gradient Approximation (GGA) in Perdew-Burke-Ernzerhof (PBE) functional are employed to deal with the exchange-correlation effect. Geometrical optimization was conducted to refine the geometry of the 3D periodic system of both materials in order to achieve a stable structure. This crucial phase was completed by reducing the total energy of the structures. Geometrical optimization of $LiTi_2(PO_4)_3$ performed at 2.471×10^{-5} eV/Atom,1.5564×10^{-2} eV/A, 3.7992×10^{-2} GPa, 3.6972×10^{-3} A for convergence, force stress, and displacement, respectively. However, during the optimization of the geometry of $Mg_{0.5}Ti_2(PO_4)_3$, the convergence of 4.4654×10^{-6} eV/Atom, a force of 6.2744×10^{-3} eV/A, stress component of 5.2283×10^{-2} GPa, and displacement of 1.1796×10^{-3} A were employed. All first-principles calculations use an ultrasoft pseudopotential, which means that only valence electrons are considered. The energy cut-off was established at 500 eV, and the Monkhorst-pack k-point grid of 4x4x4 was employed for optimization in the First Brillouin zone. The plane-wave cut-off and number of k-point were varied to verify total energy convergence.

3. RESULT AND DISCUSSION

$LiTi_2(PO_4)_3$ has a rhombohedral structure with a lattice parameter of $a = b$ = 8.534 Å and c = 20.457 Å [24]. According to Rietveld refinement analysis, $Mg_{0.5}Ti_2(PO_4)_3$ has a hexagonal structure with lattice parameter of $a = b$ = 8.4981Å and c = 20.9746 Å [25]. In this study, the primitive unit cell of LTP and MTP was chosen for geometrical optimization. Table 1 displays the lattice parameter. The crystal structure is illustrated in **Fig.1** and **Fig. 2,** respectively. Standard reference, experimental results of primitive cells that did not undergo geometrical optimization were compared to the calculated lattice constants (percentage differences were calculated). As a result of the calculation, LTP and MTP calculated by LDA-CAPZ and GGA-PBE individually show the lowest percentage difference, implying that the calculated lattice constant obtained is closer to the standard reference than other functionals. This result demonstrated that LDA-CAPZ and GGA-PBE agree with the standard reference. MTP also has a shorter lattice constant than LTP, attributed to its smaller ionic size.

Table 1. Lattice constant of LTP and MTP using three different functionals (LDA-CAPZ, GGA-PBE, and GGA-PBESOL).

		LDA-CAPZ	GGA-PBE	GGA-PBESOL	Standard reference
Lattice parameter (Å) $a = b = c$	LTP	8.4038	8.6387	8.5564	8.4128
	MTP	8.3462	8.552	8.4762	8.5413

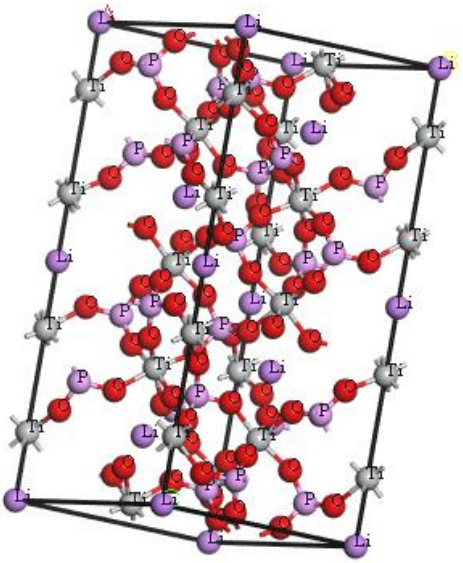

Figure 1. Crystal structure of $LiTi_2(PO_4)_3$.

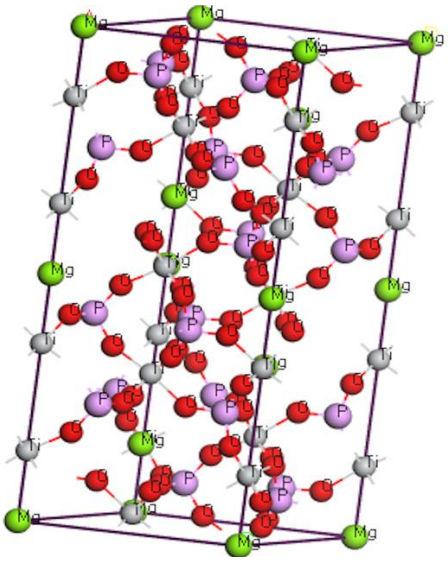

Figure 2. Crystal structure of $Mg_{0.5}Ti_2(PO_4)_3$.

LTP and MTP electronic properties are computed using the exact exchange-correlation functional, which agrees with standard reference, LDA-CAPZ, and GGA-PBE**. Fig. 3** depicts the energy band structure of LTP, while **Fig. 4** shows the energy band structure of MTP. It is observed that both materials have a direct bandgap since the bottom of the conduction band and the top of the valence band are located at the same point denoted as E_g. The calculated value of the electronic band gap is 0.10631 eV for LTP and 0.089251 eV for MTP.

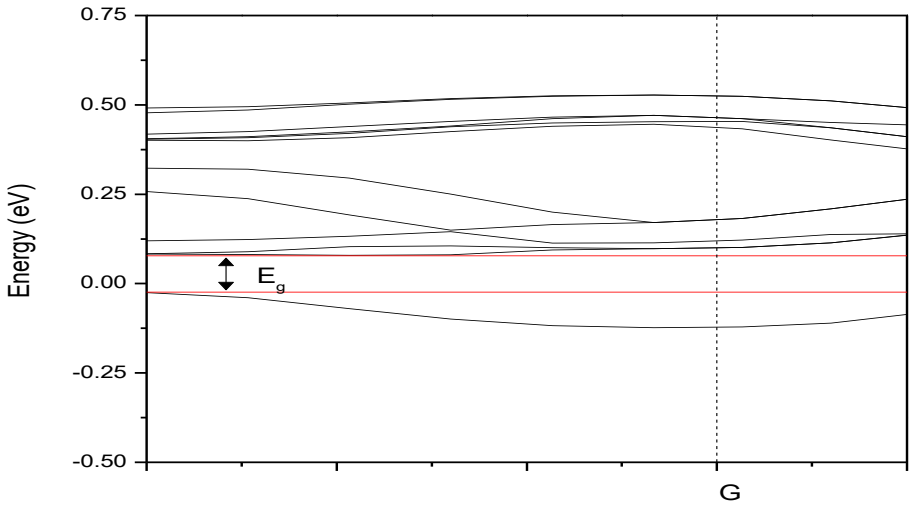

Figure 3. Electronic band structure of LTP along the symmetry axes of Brillouin zone of LDA-CAPZ $LiTi_2(PO_4)$.

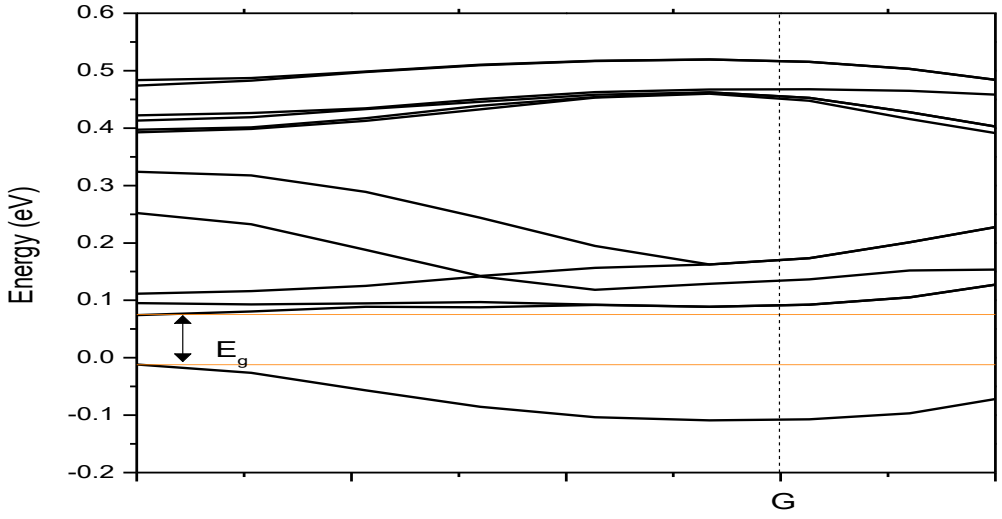

Figure 4. Electronic band structure of MTP along the symmetry axes of Brillouin zone of GGA-PBE $Mg_{0.5}Ti_2(PO_4)_3$.

The electronic density of states (DOS) represents the distribution of electrons in an energy spectrum. As an energy function, it is useful to determine the spacing between the energy band and the general distribution of states. It is represented by alpha and beta, which indicate the contribution of spin up and spin down in the plot. The position of Fermi energy is represented by a dashed line, and its value is 0 eV. In **Fig. 5**, the highest value of LTP energy in the conduction band is 3.3447 eV, whereas it is -3.3870 eV in the valence band. A study stated that LTP shows semiconductor-like electronic

conductivity by hinting electron hopping intrinsically, making it suitable for solid electrolytes [22]. **Fig. 6** portrays the density of MTP states. The highest energy value in the conduction band is 0.0473 eV, whereas the highest value in the valence band is -6.640 eV.

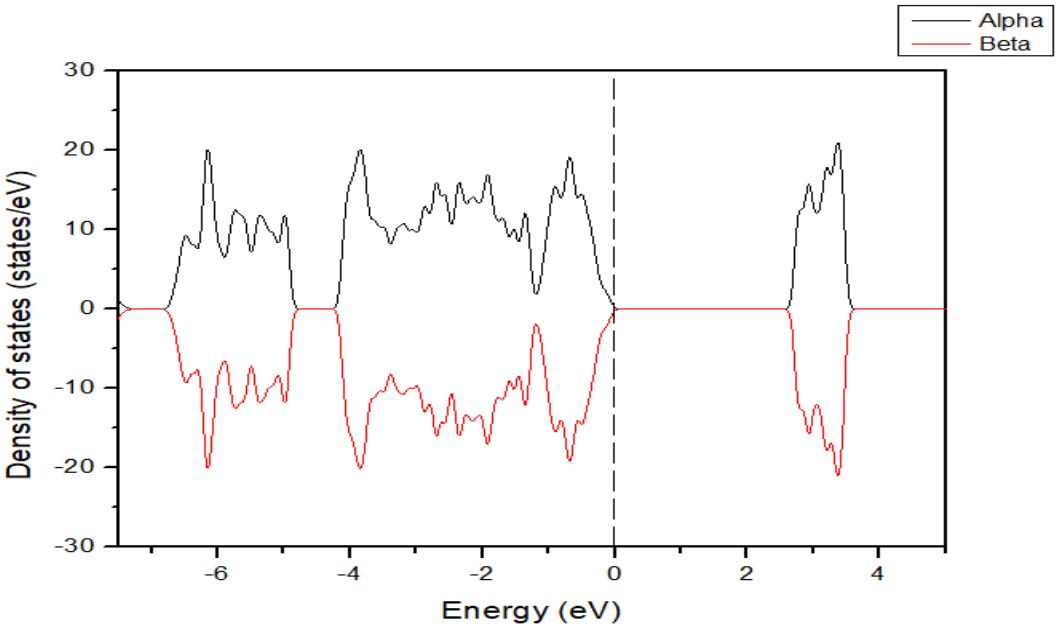

Figure 5. Density of states of $LiTi_2(PO_4)_3$.

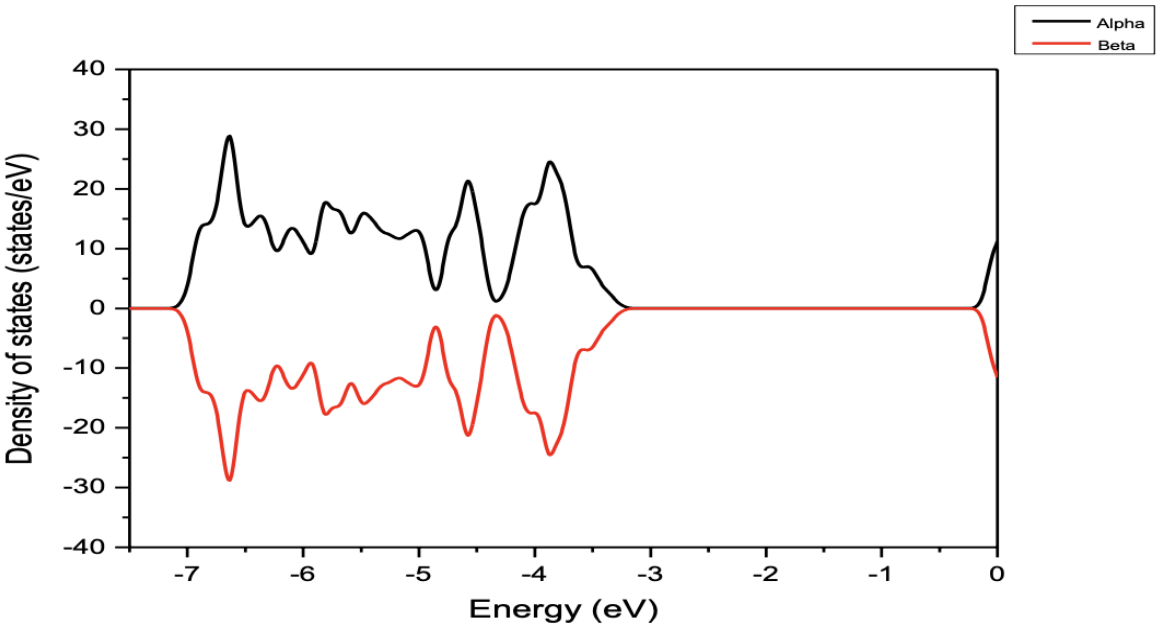

Figure 6. Density of states of $Mg_{0.5}Ti_2(PO_4)_3$.

The partial density of LTP states is calculated and illustrated in **Fig. 7**. It shows the contribution of atoms to the valence bands and conduction bands. The dashed line indicates Fermi energy, which is centered at 0 eV. Electronic states in the range of -8.75 to 0.00 eV, known as valence

band, are mainly occupied by O 2p states and less contribution from Ti 3d states. Then, there is also the contribution of Ti 3d states, P 3p states, and O 2p states in the electronic range of -2.5 to 0.00 eV. For conduction band in the range of 0.00 to 5.00 eV, it had been affected by constant contribution of Ti 3d states and few contributions from P 3p states. In addition, there are occupied by O 2p states when the energy is at 2.5 eV.

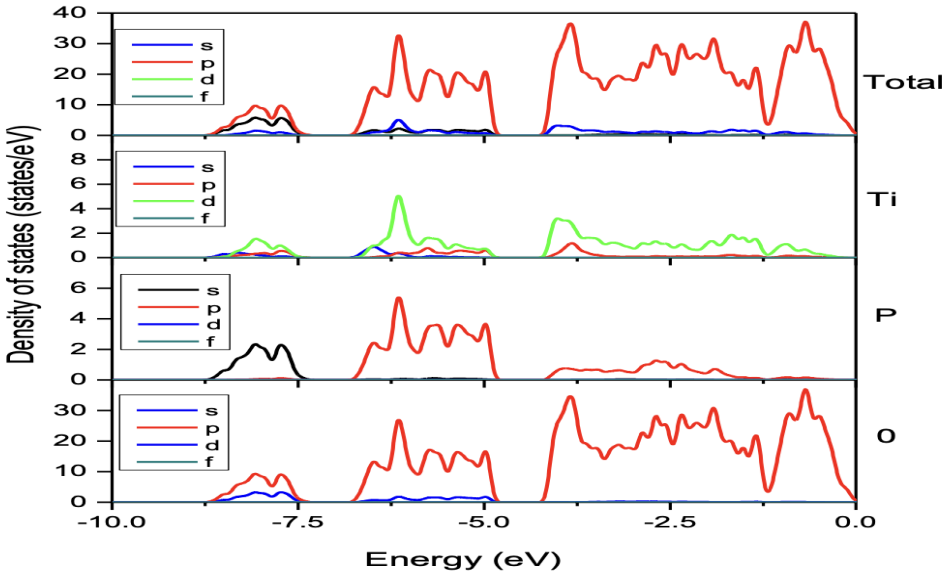

Figure 7. Partial density of states of $LiTi_2(PO_4)_3$.

4. CONCLUSION

In this study, the structural and electronic properties of $LiTi_2(PO_4)_3$ and $Mg_{0.5}Ti_2(PO_4)_3$ are explored using first-principles calculations. When the exchange-correlation functionals were compared, the LDA and GGA-PBE functionals exhibited the smallest deviation and the best agreement with standard reference. The electronic band structures of $LiTi_2(PO_4)_3$ and $Mg_{0.5}Ti_2(PO_4)_3$ are calculated, and the energy band gap obtained is 0.10631702 eV and 0.089251 eV, respectively. The electronic density of states (DOS) is determined, and the contribution of spin up (alpha) and spin down (beta) in the plot is illustrated. Partial density of states of $LiTi_2(PO_4)_3$ shows that Ti 3d, P 3p, and 0 2p states contribute significantly to the valence band. In the conduction band, there is a large contribution from Ti 3d and O 2p states. This study indicated that $Mg_{0.5}Ti_2(PO_4)_3$ is a better and more promising choice as magnesium has a higher theoretical volume energy density and does not develop dendrite, which is safer than lithium. Aside from that, $Mg_{0.5}Ti_2(PO_4)_3$ also has a more extended lattice parameter and better ion mobility, implying higher conductivity, which is an essential requirement for a suitable solid electrolyte selection. A comprehensive computational investigation related to this study should be conducted further by researchers to ensure and confirm that $Mg_{0.5}Ti_2(PO_4)_3$ is a better choice and replacement for $LiTi_2(PO_4)_3$.

ACKNOWLEDGEMENT
The authors would like to extend their gratitude towards Universiti Teknologi MARA (UiTM) for allowing this research to be carried out and for providing Grant Bestari Perdana [600-IRMI/PERDANA 5/3 BESTARI (108/2018)] in completing this study.

References

1. M. K. Khawaja, A. Alkhalidi and S. Mansour, *J. Energy Storage*, 26 (2019) 100919.
2. Y. Du, K. Fujita, S. Shironita, Y. Sone, E. Hosono, D. Asakura, M. Umeda, *J. Power Sources*, 501 (2021) 230005.
3. L. C. Yang, Q. T. Qu, Y. Shi, Y. P. Wu and T. Van Ree, Materials for lithium ion batteries by mechanochemical methods, *High-Energy Ball Milling:Mechanomical Processing of Nanopowders*, Woodhead Publishing, (2010) United Kingdom.
4. N. Nitta, F. Wu, J. T. Lee and G. Yushin, *Mater. Today*, 18 (2015) 252.
5. S. Lou, Z. Yu, Q. Liu, H. Wang, M. Chen and J. Wang, *Chem*, 6 (2020) 2199.
6. R. Dominko, J. Bitenc, R. Berthelot, M. Gauthier, G. Pagot and V. Di Noto, *J. Power Sources*, 478 (2020) 229027.
7. S. Rashidi, J. A. Esfahani and F. Hormozi, Classification of Porous Material for Energy Application, *Reference Module in Materials Science and Materials Engineering*, Elsevier (2020).
8. T. R. Crompton, *Battery Reference book*, Newnes, (2000) United Kingdom.
9. N. A. Wahab, N. A. Dzulkurnain, N. A. Mustaffa, and N. S. Mohamed, *Sci. Res. J*., 17 (2020) 191.
10. J. Schnell, T. Günther, T. Knoche, C. Vieider, L. Köhler, A. Just, M. Keller, S. Passerini and G. Reinhart, *J. Power Sources* 382 (2018) 160.
11. R. Mohtadi and F. Mizuno, *Beilstein J Nanotechnol*., 5 (2014) 1291.
12. K. Makino, Y. Katayama, T. Miura and T. Kishi, *J. Power Sources*, 99 (2001) 66.
13. Z. Guo, S. Zhao, T. Li, D. Su, S. Guo and G. Wang, *Adv. Energy Mater*., 10 (2020) 1903591.
14. P. Yadav and M. C. Bhatnagar, *J. Electroceram*., 30 (2012) 145.
15. P. Saha, M. K. Datta, O. I. Velikokhatnyi, A. Manivannan, D. Alman and P. N.Kumta, *Prog. in Mater Sci.*, 66 (2014) 1.
16. X. Lu, S. Wang, R. Xiao, S. Shi, H. Li and L. Chen, *Nano Energy*, 41 (2017) 626.
17. J. Wang, Y. Wang, D. H. Seo, T. Shi, S. Chen, Y. Tian, H. Kim and G. Ceder, *Adv. Energy Mater*., 10 (2020) 1903968.
18. Z. Jian, Y. S. Hu, X. Ji and W. Chen, *Adv. Mater*., 29 ((2017) 1601925.
19. H. Takahashi and H. Takamura, *Materials Transactions*, 53 (2012) 932.
20. Y. Zhao, Z. Wei, Q. Pang, Y. Wei, Y. Cai, Q. Fu, F. Du, A. Sarapulova, H.Ehrenberg, B. Liu and G. Chen, *ACS Appl. Mater. Interfaces*, 9 (2017) 4709.
21. G. Nuspl, T. Takeuchi, A. Weiß, H. Kageyama, K. Yoshizawa and T. Yamabe, *J. Appl. Phys*., 86 (1999) 5484.
22. N. K. Anuar, S. B. R. S. Adnan and N. S. Mohamed, *Ceram. Int*., 40 (2014) 13719.
23. L.-J. Chen, Y.-J. Zhao, J.-Y. Luo and Y.-Y. Xia, *Phys. Lett*. A, 375 (2011) 934.
24. N. A. Mustaffa and N. S. Mohamed, *Int. J. Electrochem. Sci*.,10 (2015) 5382.
25. S. Barth, R. Olazcuaga, P. Gravereau, P. Le Flem and P. Hagenmuller, *Mater. Lett*., 16 (1993) 96.